INTERNATIONAL JOURNAL FOR NUMERICAL METHODS IN FLUIDS, VOL. 3, 137–163 (1983)

A FINITE ELEMENT METHOD FOR HIGH REYNOLDS NUMBER VISCOUS FLUID FLOW USING TWO STEP EXPLICIT SCHEME

MUTSUTO KAWAHARA

Department of Civil Engineering, Chuo University Kasuga, Bunkyo-ku, Tokyo, 112, Japan

AND

HIROKAZU HIRANO

Mitsui Engineering and Shipbuilding Co., Ltd. Tsukiji, Chuo-ku, Tokyo, 104, Japan

SUMMARY

This paper presents the finite element method for the analysis of unsteady viscous flow of fluid at high Reynolds numbers. The method is based on the explicit numerical integration scheme in time and uses three node triangular finite elements. For the convenience of the formulation, slight compressibility is considered. For the explicit scheme, the selective lumping two step scheme has been successfully employed. Vortex shedding behind a cylinder has been computed and compared with the conventional experimental results. The results agree favourably when both schemes are compared.

KEY WORDS Selective Lumping Scheme High Reynolds Number Vortex Shedding

1. INTRODUCTION

Recent developments of the finite element method have demonstrated that it is one of the most successful numerical methods for the analysis of incompressible viscous flow. The method is particularly adaptable for the analysis of both steady and unsteady flow. The main objective of the current work is to overcome the difficulty that the fluid is incompressible. One of the promising methods, referred to as the penalty function method, has been investigated by a number of researchers.

Relatively high Reynolds number flow has been solved by the penalty function method. Hughes *et al.*[1,2] have presented the steady flow analysis based on rectangular finite elements and on a reduced integration scheme. Heinrich *et al.*[3] have discussed the formulation on the quadratic interpolation equation. Mathematical aspects of reduced integration have been dealt with Reddy[4,5] and Oden.[6] Temam[7,8] has presented the mathematical convergence of the penalty function method for unsteady flow but without numerical illustration. Lee *et al.*[9,10] and Gresho *et al.*[11] have investigated the steady and unsteady penalty function method. They presented numerical results for a Reynolds number of $1{\cdot}0 \times 10^5$. Because their formulation is based on the implicit type of numerical integration in time, the refinement of the finite element idealization seems rather insufficient.

The basic idea of the penalty function method can be found in the classical finite difference analysis, for instance, References 12–14. The ideas in those papers are closely related to those of artificial compressibility. The fluid existing in the natural world is not strictly

0271–2091/83/020137–27$02.70

Received 6 October 1981
Revised 4 May 1982

incompressible, i.e. observations always show that the propagating speed of sound through the fluid has a finite value. It could be stated that the conventional analysis can be performed for the idealized material which in fact, could not exist in the natural world.

This paper presents the finite element analysis for fluid flow including compressibility, i.e. a finite value of the speed of sound. The improved equation of continuity is derived from equations of both state and conservation of mass. If the speed of sound in the improved equation tends to infinity, the equation becomes coincident with the conventional equation of continuity. This is also the physical interpretation of the penalty function method.

In the conventional finite element method, the implicit type of numerical integration scheme in time is usually used. One of the reasons for this is that the equation of continuity for incompressible flow is independent of the *timewise* derivative of pressure. It is, then, practically impossible to apply the explicit type of numerical integration scheme. However, the diagonal terms of the coefficient matrix to be solved in the implicit scheme include some zero values, which drastically reduces the conditioning of the simultaneous equation system. In particular, the zero value in the diagonal terms reduce the stability of solution of the simultaneous equations.

The time increment in the implicit scheme can be taken longer than that of the explicit scheme. The computation of the implicit scheme may be more stable than that of the explicit scheme. Regardless of these facts, this paper concentrates on presenting the finite element method based on the explicit numerical integration scheme in time. The reason is as follows. It is necessary to use extremely refined finite element idealization to compute the flow at high Reynolds numbers. To solve the simultaneous equations, a large size of computer core storage is required. But, even if the largest scale computer could be available, the core storage capacity would still be great. Contrary to this, if the explicit method is used, the computer core storage can be drastically reduced. This is because only the core storage for the coefficient data of each finite element is required in the explicit computation. The explicit integration can be carried out by the simple operations of multiplication in an element-wise manner. To pursue the complicated phenomena at high Reynolds number, e.g. vortex shedding behind an obstacle, a substantially short time increment should be essential. In this sense, the explicit scheme is more useful. Total computational time is also saved even if the time increment is limited by the travelling time of sound through the minimum length of each finite element.

The numerical test examples have been performed for the comparison with the analytical solutions and the numerical solution obtained by Lee *et al.*[9] Generally, both numerical and analytical results are in close agreement. These examples have illustrated that the present method is adaptable for the computation of incompressible fluid flow. For the practical applications, vortex shedding behind a cylinder has been analysed using the present method. The computed velocity shows the behaviour of vortex production and separation quite clearly. The Strouhal number is compared with the experimental result. Both results are in agreement. The pressure coefficient around the cylinder is compared with experimental values. In an average sense, both results are reasonably coincident. From the numerical experiments described in this paper, it is concluded that the present finite element method is one of the most practically suitable methods for the analysis of the fluid flow at high Reynolds numbers.

2. BASIC EQUATIONS

The aim of this paper is to present the finite element method to solve a two dimensional transient flow of an incompressible viscous fluid. Extensions to the analysis of a three

dimensional flow or thermally conductive flow are simple and straightforward. In the process of the analysis, the compressibility of the fluid is considered. The basic equations employed are summarized in this section.

Indicial notation and the usual summation convention with repeated indices are introduced to describe the equations. The spatial rectangular co-ordinate system x_i $(i=1,2)$ is used. Notations $(\ )_{,i}$ and $(\cdot)$ mean partial differentiation with respect to co-ordinate, x_i, and time, t, respectively. The Kronecker delta function is expressed by δ_{ij}.

Introducing density of fluid ρ and velocity u_i, the conservation law of mass can be expressed as follows.

$$\frac{\partial \rho}{\partial t}+(\rho u_i)_{,i}=0 \tag{1}$$

Using the conservation law of linear momentum, the equation of motion is derived as:

$$\rho\left(\frac{\partial u_i}{\partial t}+u_j u_{i,j}\right)+p_{,i}-\tau_{ij,j}+\rho f_i=0 \tag{2}$$

where p, τ_{ij}, f_i denote pressure, viscous stress and body force, respectively. The viscous stress is assumed to be written as a function of velocity gradient as:

$$\tau_{ij}=\kappa d_{kk}\delta_{ij}+2\mu d_{ij} \tag{3}$$

where κ and μ represent volumetric and shear viscous coefficients, respectively, and the deformation rate d_{ij} is described as:

$$d_{ij}=\tfrac{1}{2}(u_{i,j}+u_{j,i}) \tag{4}$$

Since the pressure is a function of density the equation of state can be expressed in the following form.

$$p=p(\rho) \tag{5}$$

Using this, the speed of sound, c, is defined as:

$$c^2=\frac{\partial p}{\partial \rho} \tag{6}$$

The speed of sound can be taken as a constant since the incompressible flow is being considered.

Regarding boundary conditions, the following four types of conditions will be considered. The velocity is assumed to be prescribed on boundary S_1, i.e.

$$u_i=\hat{u}_i, \quad \text{on } S_1 \tag{7}$$

where superposed $\hat{}$ means the prescribed function on the boundary. The surface force is supposed to be given on boundary S_2, i.e.

$$s_i=(-p\,\delta_{ij}+\tau_{ij})n_j=\hat{s}_i, \quad \text{on } S_2 \tag{8}$$

where n_j is a unit normals to the boundary. The surface flux condition will be denoted by;

$$t_i=\tau_{ij}n_j=\hat{t}_i, \quad \text{on } S_3 \tag{9}$$

The pressure is enforced on boundary S_4 as

$$p=\hat{p}, \quad \text{on } S_4 \tag{10}$$

Finally, the discharge is written on boundary S_5 as follows,

$$q = u_i n_i = \hat{q}, \quad \text{on } S_5 \tag{11}$$

This paper deals with two cases, denoted analysis I and analysis II. In analysis I, the velocity condition is considered as the essential boundary condition and the surface force is as the natural boundary condition. For this purpose, the following assumption is introduced

$$\begin{aligned} S_1 \cup S_2 &= S \\ S_1 \cap S_2 &= \varnothing \end{aligned} \tag{12}$$

where S denotes whole boundary and $\varnothing$ is a null set. Equation (12) means that the whole boundary consists of two boundaries only, on which velocity and surface force are prescribed, and these boundaries are not overlapped.

In analysis II, the velocity and pressure conditions are taken as the essential boundary conditions and the surface flux and discharge are as the natural boundary conditions. For this purpose, the following assumptions are used.

$$\begin{aligned} S_1 \cup S_3 &= S \\ S_1 \cap S_3 &= \varnothing \end{aligned} \tag{13}$$

$$\begin{aligned} S_4 \cup S_5 &= S \\ S_4 \cap S_5 &= \varnothing \end{aligned} \tag{14}$$

Equation (13) means that the whole boundary consists of two boundaries only, on which velocity and surface flux are prescribed, and these boundaries are not overlapped. Equation (14) also means that the whole boundary consists of two boundaries only, on which pressure and discharge are prescribed, and these boundaries are not overlapped.

The essential difference between analyses I and II is centered on the description of pressure. In analysis I, the pressure is described as the natural boundary condition, whereas the pressure is itself given as the essential boundary condition in analysis II.

3. TRANSFORMATION OF THE BASIC EQUATIONS

Equations (1)–(4) are referred to as the basic equations in this paper. These equations can be transformed into more suitable forms for the explicit finite element method. Since the compressibility is nearly insignificant, the density of fluid ρ can be taken as a constant with respect to co-ordinate x_i and time t in a part of the transformation process. Non-dimensional forms can also be derived.

Differentiating both sides of equation (5), the equation of state is reformulated as follows.

$$\frac{Dp}{Dt} = \frac{\partial p}{\partial \rho} \frac{D\rho}{Dt} \tag{15}$$

where D/Dt means the material derivatives with respect to time, t. Using equations (1) and (6), the following equation is derived from equation (15).

$$\frac{\partial p}{\partial t} + u_i p_{,i} + \rho c^2 u_{i,i} = 0 \tag{16}$$

If the speed of sound tends to infinity, equation (16) becomes the well known equation of continuity.

$$u_{i,i} = 0 \tag{17}$$

Almost all of the previously published finite element methods have employed equation (17) as the equation of continuity. Contrary to this, it is inconvenient to formulate the explicit finite element method using equation (17). Therefore, in this paper equation (16) is used as the equation of continuity since the explicit finite element method can be formulated quite readily based on this equation.

Introducing equations (3) and (4) into equation (2) and rearranging the terms, the following equation of motion is derived.

$$\rho\left(\frac{\partial u_i}{\partial t}+u_j u_{i,j}\right)+p_{,i}-\kappa u_{k,ki} -\mu(\mu_{i,j}+\mu_{j,i})_{,j}+\rho f_i=0 \tag{18}$$

in which the volumetric viscous coefficient κ is introduced since the equation includes compressibility. However, since the method aims to solve the incompressible flow, the volumetric coefficient κ will be set to zero.

Taking the reference length L and velocity U, the non-dimensional time and co-ordinate are introduced as:

$$T=\frac{tL}{U}, \qquad X_i=\frac{x_i}{L} \tag{19), (20}$$

Using equations (19) and (20), the non-dimensional form of the equation of momentum is derived as follows.

$$\frac{\partial v_i}{\partial t}+v_j v_{i,j}+CP_{,i}-\lambda v_{k,ki} -\nu(v_{i,j}+v_{j,i})_{,j}+F_i=0 \tag{21}$$

where

$$v_i=\frac{u_i}{U}, \qquad P=\frac{p}{\rho cU}, \qquad \lambda=\frac{\kappa}{\rho UL}$$

$$\nu=\frac{\mu}{\rho UL}=\frac{1}{Re}, \qquad C=\frac{c}{U}=\frac{1}{Mc}$$

$$F_i=\frac{Lf_i}{U}$$

Using equations (19) and (20), the non-dimensional form of the equation of continuity is obtained as follows.

$$\frac{\partial P}{\partial t}+v_i P_{,i}+Cv_{i,i}=0 \tag{22}$$

The finite element analysis in this paper will be formulated based on equations (21) and (22).

Boundary conditions for analysis I are

$$\begin{aligned} &v_i=\hat{v}_i, && \text{on } S_1\\ &S_i=(-CP\delta_{ij}+t_{ij})n_j=\hat{S}_i, && \text{on } S_2 \end{aligned} \tag{23}$$

where

$$S_i=\frac{s_i}{\rho U}$$

In an almost similar manner, boundary conditions for analysis II are written as follows.

$$\begin{aligned} v_i &= \hat{v}_i, && \text{on } S_1 \\ T_i &= t_{ij}n_j = \hat{T}_i, && \text{on } S_3 \end{aligned} \tag{24}$$

$$\begin{aligned} P &= \hat{P}, && \text{on } S_4 \\ Q &= Cv_in_i = \hat{Q}, && \text{on } S_5 \end{aligned} \tag{25}$$

where

$$T_i = \frac{t_i}{\rho U}, \qquad t_{ij} = \frac{\tau_{ij}}{\rho U}, \qquad Q = C\frac{q}{U}$$

4. WEIGHTED RESIDUAL EQUATIONS

As the first step of the finite element method, it is necessary to introduce the weighted residual equations. Let v_i^* be the weighting function for velocity, the value of which is arbitrary except on boundary S_1, where it takes a value of zero. Multiplying both sides of equation (21) by v_i^* and integrating over the volume V, the following equation is derived.

$$\begin{aligned} &\int_V \left(v_i^* \frac{\partial v_i}{\partial t}\right) dV + \int_V (v_i^* v_j v_{i,j})\, dV + \int_V (v_i^* C P_{,i})\, dV \\ &\quad - \int_V (v_i^* \lambda v_{k,ki})\, dV - \int_V \{v_i^* \nu (v_{i,j} + v_{j,i})\}\, dV \\ &\quad + \int_V (v_i^* f_i)\, dV = 0 \end{aligned} \tag{26}$$

Let P^* be the weighting function for pressure, the value of which is arbitrary except on boundary S_3, where it takes a value of zero. Multiplying both sides of equation (22) by P^*, and integrating over the volume V, the following equation is obtained.

$$\int_V \left(P^* \frac{\partial P}{\partial t}\right) dV + \int_V (P^* v_i P_{,i})\, dV + \int_V (P^* C v_{i,i})\, dV = 0 \tag{27}$$

In analysis I, the weighted residual equation is derived using integration by parts on equation (26).

$$\begin{aligned} &\int_V \left(v_i^* \frac{\partial v_i}{\partial t}\right) dV + \int_V (v_i^* v_j v_{i,j})\, dV - C\int_V (v_{i,i}^* P)\, dV \\ &\quad + \lambda \int_V (v_{i,i}^* v_{k,k})\, dV + \nu \int_V (v_{i,j}^* v_{i,j})\, dV \\ &\quad + \nu \int_V (v_{i,j}^* v_{j,i})\, dV + \int_V (v_i^* F_i)\, dV \\ &\quad = \int_{S_2} (v_i^* \hat{S}_i)\, dS \end{aligned} \tag{28}$$

In the derivation of equation (28), equations (12) and (23) are used. Equation (28) includes the surface force boundary condition on S_2 as the natural boundary condition. In analysis I, equations (27) and (28) with the essential boundary condition for velocity are used as the weighted residual equation.

In analysis II, the weighted residual equation is obtained using integration by parts on equation (26).

$$\int_V \left(v_i^* \frac{\partial v_i}{\partial t}\right) \mathrm{d}V + \int_V (v_i^* v_j v_{i,j}) \,\mathrm{d}V + C\int_V (v_i^* P_{,i}) \,\mathrm{d}V + \lambda\int_V (v_{i,i}^* v_{k,k}) \,\mathrm{d}V + \nu\int_V (v_{i,j}^* v_{i,j}) \,\mathrm{d}V + \nu\int_V (v_{i,j}^* v_{j,i}) \,\mathrm{d}V + \int_V (v_i^* F_i) \,\mathrm{d}V = \int_{S_3} (v_i^* \hat{T}_i) \,\mathrm{d}S \tag{29}$$

In the derivation of equation (29), equations (13) and (24) are used. Equation (29) includes the surface flux boundary condition on S_3 as the natural boundary condition. Integration by parts of equation (27) leads to the following equation.

$$\int_V \left(P^* \frac{\partial P}{\partial t}\right) \mathrm{d}V + \int_V (P^* v_i P_{,i}) \,\mathrm{d}V - \int_V (P_{,i}^* C v_i) \,\mathrm{d}V = \int_{S_5} (P^* \hat{Q}) \,\mathrm{d}S \tag{30}$$

In the derivation of equation (30), equations (14) and (25) are employed. Equation (30) includes the surface flux boundary condition on S_5 as the natural boundary condition. In analysis II, equations (29) and (30) with the essential boundary condition for velocity and pressure are used for the weighted residual equation.

5. FINITE ELEMENT ANALYSIS

It is supposed that the flow field to be analysed is divided into a large number of small domains called finite elements. Both trial and weighting functions are assumed in the following manner. For velocity, the interpolation equation is:

$$v_i = \Phi_\alpha v_{\alpha i} \tag{31}$$

$$v_i^* = \Phi_\alpha v_{\alpha i}^* \tag{32}$$

where Φ_α is the interpolation function, $v_{\alpha i}$ represents the nodal value of velocity at the αth node of the finite element in the ith direction and $v_{\alpha i}^*$ is the nodal value of the corresponding weighting function, respectively. For pressure, the interpolation equation is:

$$P = \Phi_\alpha P_\alpha \tag{33}$$

$$P^* = \Phi_\alpha P_\alpha^* \tag{34}$$

where P_α denotes the nodal value of pressure at αth node of the finite element and P_α^* is the nodal value of the corresponding weighting function, respectively. The interpolation function is essentially related to the stability of a numerical integration scheme in time. Taking the fact into account that the present method employs the two step explicit scheme for the numerical integration in time, the linear interpolation function based on three node triangular finite element is used for both velocity and pressure.

Substituting equations (31)–(34) into equations (27) and (28), considering the arbitrariness of $v_{\alpha i}^*$ and P_α^* and rearranging the terms, the finite element equation for analysis I can be

derived as follows.

$$M_{\alpha\beta}\dot{v}_{\beta j} + K_{\alpha\beta\gamma j}v_{\beta j}v_{\gamma i} + H_{\alpha i\beta}P_\beta + S_{\alpha i\beta j}v_{\beta j} = \hat{\Omega}_{\alpha i} \tag{35}$$

$$M_{\alpha\beta}\dot{P}_\beta + A_{\alpha\beta i}P_\beta v_{\gamma i} + B_{\alpha\beta i}v_{\beta i} = \hat{\Sigma}_\alpha \tag{36}$$

where

$$M_{\alpha\beta} = \int_V (\Phi_\alpha \Phi_\beta)\,\mathrm{d}V$$

$$K_{\alpha\beta\gamma j} = \int_V (\Phi_\alpha \Phi_\beta \Phi_{\gamma,j})\,\mathrm{d}V$$

$$H_{\alpha i\beta} = -C\int_V (\Phi_{\alpha,i}\Phi_\beta)\,\mathrm{d}V$$

$$S_{\alpha i\beta j} = \lambda\int_V (\Phi_{\alpha,i}\Phi_{\beta,j})\,\mathrm{d}V + \nu\int_V (\Phi_{\alpha,i}\Phi_{\beta,j})\,\mathrm{d}V + \nu\int_V (\Phi_{\alpha,k}\Phi_{\beta,k})\,\delta_{ij}\,\mathrm{d}V$$

$$\hat{\Omega}_{\alpha i} = \int_{S_2} (\Phi_\alpha S_i)\,\mathrm{d}S - \int_V (\Phi_\alpha F_i)\,\mathrm{d}V$$

$$A_{\alpha\beta i\gamma} = \int_V (\Phi_\alpha \Phi_{\beta,i}\Phi_\gamma)\,\mathrm{d}V$$

$$B_{\alpha\beta i} = C\int_V (\Phi_\alpha \Phi_{\beta,i})\,\mathrm{d}V$$

$$\hat{\Sigma}_\alpha = 0$$

Introducing equations (31)–(34) into equations (29) and (30), considering the arbitrariness of $v^*_{\alpha i}$ and P^*_α and rearranging the terms, the finite element equation for analysis II can be derived in the same forms of equations (35) and (36), where

$$H_{\alpha i\beta} = C\int_V (\Phi_\alpha \Phi_{\beta,i})$$

$$\hat{\Omega}_{\alpha i} = \int_{S_3} (\Phi_\alpha \hat{T}_i)\,\mathrm{d}S - \int_V (\Phi_\alpha F_i)\,\mathrm{d}V$$

$$B_{\alpha\beta i} = -C\int_V (\Phi_{\alpha,i}\Phi_\beta)\,\mathrm{d}V$$

$$\hat{\Sigma}_\alpha = \int_{S_5} (\Phi_\alpha \hat{Q})\,\mathrm{d}S$$

Henceforth, equations (35) and (36) are regarded as the finite element equations for both analysis I and analysis II. The finite element equation for the whole flow field is also derived in the same form as in equations (35) and (36).

For the numerical integration in time, the selective lumping two step explicit method is effectively used. The method has already been investigated by Kawahara *et al.*[15–23] The numerical integration procedure consists of two steps and can be applied to equations (35) and (36) as follows.

For the first step:

$$\bar{M}_{\alpha\beta}v_{\beta i}^{n+\frac{1}{2}} = \bar{M}_{\alpha\beta}v_{\beta i}^{n} - \frac{\Delta t}{2}(K_{\alpha\beta\gamma j}v_{\beta j}^{n}v_{\gamma i}^{n} + S_{\alpha i\beta j}v_{\beta_i}^{n} + H_{\alpha i\beta}P_{\beta}^{n} + \hat{\Omega}_{\alpha_i}^{n}) \tag{37}$$

$$\bar{M}_{\alpha\beta}P_{\beta}^{n+\frac{1}{2}} = \bar{M}_{\alpha\beta}P_{\beta}^{n} - \frac{\Delta t}{2}(A_{\alpha\beta i\gamma}v_{\beta i}^{n}P_{\gamma}^{n} + B_{\alpha i\beta}v_{\beta i}^{n} + \hat{\Sigma}_{\alpha}^{n}) \tag{38}$$

and for the second step:

$$\bar{M}_{\alpha\beta}v_{\beta i}^{n+1} = \bar{M}_{\alpha\beta}v_{\beta i}^{n} - \Delta t(K_{\alpha\beta\gamma j}v_{\beta j}^{n+\frac{1}{2}}v_{\gamma i}^{n+\frac{1}{2}} + S_{\alpha i\beta j}v_{\beta j}^{n} + H_{\alpha i\beta}P_{\beta}^{n+\frac{1}{2}} + \hat{\Omega}_{\alpha i}^{n}) \tag{39}$$

$$\bar{M}_{\alpha\beta}P_{\beta}^{n+1} = \bar{M}_{\alpha\beta}P_{\beta}^{n} - \Delta t(A_{\alpha\beta i\gamma}v_{\beta i}^{n+\frac{1}{2}}P_{\gamma}^{n+\frac{1}{2}} + B_{\alpha i\beta}v_{\beta i}^{n+\frac{1}{2}} + \hat{\Sigma}_{\alpha}^{n}) \tag{40}$$

where superscripted n means the value at nth time step, $\bar{M}_{\alpha\beta}$ denotes the lumped coefficient and $\tilde{M}_{\alpha\beta}$ is

$$\tilde{M}_{\alpha\beta} = e\bar{M}_{\alpha\beta} + (1-e)M_{\alpha\beta} \tag{41}$$

in which e is referred to as the selective lumping parameter. The parameter e controls the numerical damping and the numerical stability, which has been throughly investigated by Kawahara *et al.*[22,23]

6. STABILITY CONSIDERATION

To establish the practically useful rule for the computational stability, Neumann condition is investigated for one dimensional linearized equation. Consider the following equation:

$$\frac{\partial u}{\partial t} + U\frac{\partial u}{\partial x} + C\frac{\partial P}{\partial x} - \nu\frac{\partial^2 u}{\partial x^2} = 0 \tag{42}$$

$$\frac{\partial P}{\partial t} + U\frac{\partial P}{\partial x} + C\frac{\partial u}{\partial x} = 0 \tag{43}$$

where u and P represent velocity and pressure and U, C, ν are reference velocity, sound speed, viscosity, respectively, and the latter three are assumed constant. For the ith nodal point of the equivalent mesh idealization and nth time point, the finite element equation is written as follows:

For the first step:

$$\begin{aligned} u_i^{n+\frac{1}{2}} = u_i^n &- U\frac{\mu}{2}[(-\tfrac{1}{2})u_{i-1}^n + (\tfrac{1}{2})u_{i+1}^n] \\ &- \left(\frac{\nu}{\Delta x}\right)\frac{\mu}{2}[(-1)u_{i-1}^n + (2)u_i^n + (-1)u_{i+1}^n] \\ &- C\frac{\mu}{2}[(-\tfrac{1}{2})P_{i-1}^n + (\tfrac{1}{2})P_{i+1}^n] \end{aligned} \tag{44}$$

$$\begin{aligned} P_i^{n+\frac{1}{2}} = (\tfrac{1}{6})P_{i-1}^n &+ (\tfrac{2}{3})P_i^n + (\tfrac{1}{6})P_{i+1}^n \\ &- U\frac{\mu}{2}[(-\tfrac{1}{2})P_{i-1}^n + (\tfrac{1}{2})P_{i+1}^n] \\ &- C\frac{\mu}{2}[(-\tfrac{1}{2})u_{i-1}^n + (\tfrac{1}{2})u_{i+1}^n] \end{aligned} \tag{45}$$

and for the second step:

$$u_i^{n+1} = u_i^n - U\mu[(-\tfrac{1}{2})u^{n+\frac{1}{2}} + (\tfrac{1}{2})u^{n+\frac{1}{2}}]$$
$$-\left(\frac{\nu}{\Delta x}\right)\mu[(-1)u_{i-1}^n + (2)u_i^n + (-1)u_{i+1}^n]$$
$$-C\mu[(-\tfrac{1}{2})P^{n+\frac{1}{2}} + (\tfrac{1}{2})P^{n+\frac{1}{2}}] \tag{46}$$

$$P_i^{n+1} = (\tfrac{1}{6})P_{i-1}^n + (\tfrac{2}{3})P_i^n + (\tfrac{1}{6})P_{i+1}^n$$
$$-U\mu[(-\tfrac{1}{2})P^{n+\frac{1}{2}} + (\tfrac{1}{2})P^{n+\frac{1}{2}}]$$
$$-C\mu[(-\tfrac{1}{2})u^{n+\frac{1}{2}} + (\tfrac{1}{2})u^{n+\frac{1}{2}}] \tag{47}$$

where

$$\mu = \frac{\Delta t}{\Delta x}$$

in which Δx and Δt represent the distance between nodal points and the time increment, respectively. Assume that the solutions of equations (44)–(47) can be expressed as:

$$u_i^n = R^n e^{j\omega i} \tag{48}$$

$$P_i^n = Q^n e^{j\omega i} \tag{49}$$

where $j = \sqrt{-1}$. Introducing equations (48) and (49) into equations (44)–(47) and rearranging the terms, the following amplification relations can be derived.

$$\begin{pmatrix} R^{n+\frac{1}{2}} \\ Q^{n+\frac{1}{2}} \\ \hline R^{n+1} \\ Q^{n+1} \end{pmatrix} = \left(\begin{array}{cc:cc} 1-e-j\frac{U}{2}b & -j\frac{C}{2}b & & \\ -j\frac{C}{2}b & a-j\frac{U}{2}b & & \\ \hdashline 1-e & & -jUb & -jCb \\ & a & -jUb & -jCb \end{array}\right) \begin{pmatrix} R^n \\ Q^n \\ \hline R^{n+\frac{1}{2}} \\ Q^{n+\frac{1}{2}} \end{pmatrix} \tag{50}$$

where

$$a = \tfrac{2}{3} + \tfrac{1}{3}\cos\omega$$
$$b = \mu \sin\omega$$
$$e = \left(\frac{\nu}{\Delta x}\right)\mu(1-\cos\omega)$$

For the eigenvalue λ of equation (50), the following equation can be obtained.

$$\lambda(\lambda + jUb + jCb)\left\{\left(1-e-j\frac{U}{2}b-\lambda\right)\left(a-j\frac{U}{2}b-\lambda\right)+\frac{C^2b^2}{4}\right\} = 0 \tag{51}$$

From equation (51), four eigenvalues can be derived as:

$$\lambda_1 = 0 \tag{52}$$

$$\lambda_2 = -jb(U+C) \tag{53}$$

$$\lambda_3 = -\frac{Ub}{2}j + \frac{a-e+1+\sqrt{(-C^2b^2+a^2-2a+2ae+e^2-2e+1)}}{2} \tag{54}$$

$$\lambda_4 = -\frac{Ub}{2}j + \frac{a-e+1\sqrt{(-C^2b^2+a^2-2a+2ae+e^2-2e+1)}}{2} \tag{55}$$

The criterion for the selection of the time increment Δt is obtained from equation (53) in the following form.

$$\Delta t \leqq \frac{\Delta x}{U+C} \tag{56}$$

From equations (54) and (55), a similar criterion must be obtained. However, the criteria seem rather cumbersome and useless for practical computations. There is a possibility that some time increment, Δt, arbitrarily chosen could be tested to satisfy the criteria.

Aside from these, the authors' numerical experiences show that the equation:

$$\Delta t \leqq \alpha \frac{\Delta x}{U+C} \tag{57}$$

is extremely useful for the practical computation. Usually, the constant α is chosen with in the range of $0{\cdot}1 \sim 0{\cdot}3$. It is interesting that α is almost independent of viscosity.

7. TEST EXAMPLES

The first example concerns the propagation of a sound wave, i.e. the difference of pressure. This example is the test for the adaptability of the present finite element method in analysis I, especially for the choice of the selective lumping parameter. The problem will be restricted to one dimension as:

$$\frac{\partial v}{\partial T} + v\frac{\partial v}{\partial x} + C\frac{\partial P}{\partial x} = 0 \tag{58}$$

$$\frac{\partial P}{\partial T} + v\frac{\partial P}{\partial x} + C\frac{\partial v}{\partial x} = 0 \tag{59}$$

where v, P denote velocity and pressure and C is speed of sound respectively. The speed of sound is assumed a constant. Figure 1 shows the finite element idealization used in the computation. The problem is completely one dimensional. However, a two dimensional method of solution has been used in order to test the present finite element method and for the boundary condition, normal velocity on all boundaries A–B–C–D is assumed zero. For the initial condition, the pressure difference between two regions separated at the centre is enforced as $P_1 = 11$ and $P_3 = 10$.

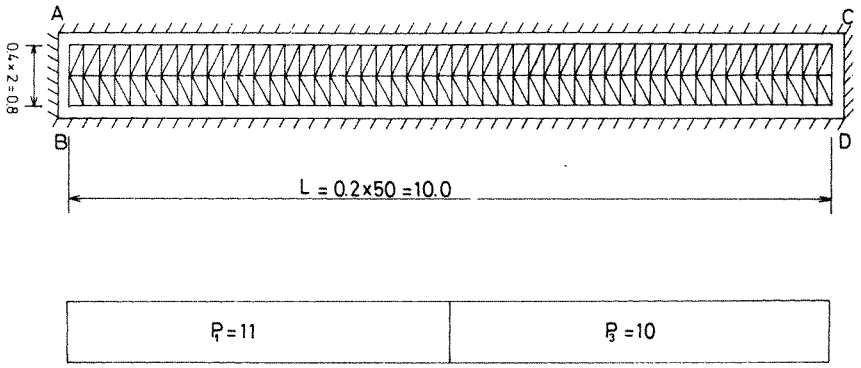

Figure 1.

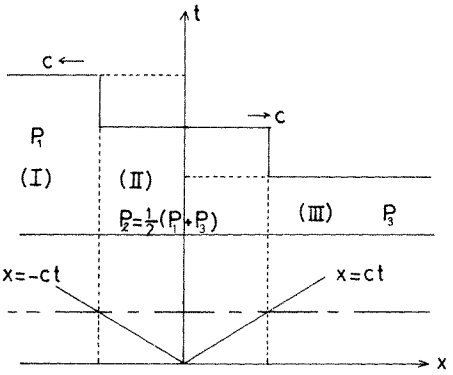

Figure 2.

From equations (58) and (59), the following conservation equation can be derived.

$$\left[\frac{\partial}{\partial T}+(v+C)\frac{\partial}{\partial x}\right](v+P)=0 \tag{60}$$

$$\left[\frac{\partial}{\partial T}+(v-C)\frac{\partial}{\partial x}\right](v-P)=0 \tag{61}$$

Therefore, $(v+P)$ and $(v-P)$ are conserved. At the wave front, the following equations are valid.

$$[\![\rho v]\!]=0 \tag{62}$$

$$\left[\!\left[P+\frac{v}{C}\right]\!\right]=0 \tag{63}$$

where ρ is density and $[\![\ ]\!]$ denotes the difference at the wave front. Using the above relations, the propagation of the sound wave can be expressed schematically as in Figure 2. The propagation speed is C and pressure at the intermediate region P_2 is derived as follows.

$$P_2=\tfrac{1}{2}(P_1+P_2) \tag{64}$$

Figure 3 illustrates the computed wave propagation of pressure using the selective lumping parameter $e=0{\cdot}7$ and sound speed $C=1000$. The initial condition is denoted by the broken line. Solid circles are for computed pressure. The propagation of a wave and the reflection of a wave have been clearly shown. The results are in close agreement with the analytical solution.

The comparison of the reflected wave with the various selective lumping parameters is represented in Figure 4. In the case where $e=0$, there seems a slight damping effect. In the case where $e=0{\cdot}95$, the computed pressure seems to include computational instability. From Figures 3 and 4, it is concluded that the wave propagation can be computed exactly using the proper choice of the selective lumping parameter. If the choice of the parameter is not suitable, the instability of the computation or the superfluous numerical damping will arise.

The second example is the computation of pressure and velocity responding to the sinusoidal variation of the pressure at the boundary. The computation has been carried out by the formulation in the analysis II. The computed results have been obtained by using the two dimensional computer program and including the non-linear terms. An analytical

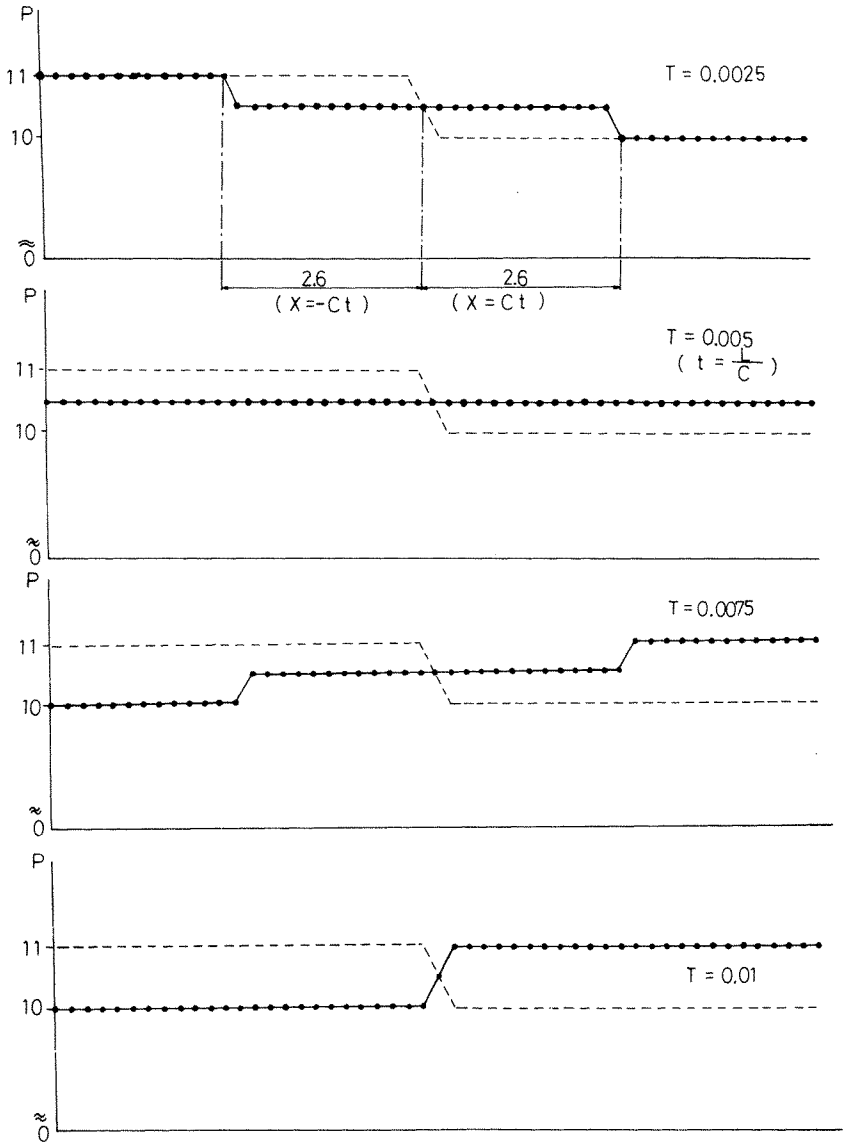

Figure 3.

solution is obtained for the linear problem:

$$\frac{\partial v}{\partial t}+C\frac{\partial P}{\partial x}=0 \tag{65}$$

$$\frac{\partial P}{\partial t}+C\frac{\partial v}{\partial x}=0 \tag{66}$$

$$P=a\sin\omega t, \quad \text{at} \quad x=x_0+L \tag{67}$$

$$\frac{\partial P}{\partial x}=0, \quad \text{at} \quad x=x_0 \tag{68}$$

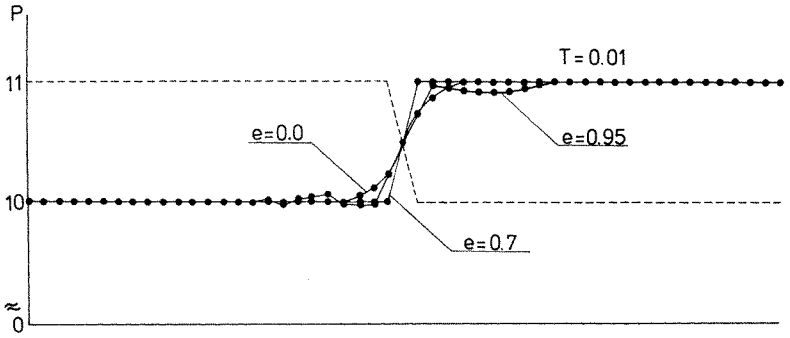

Figure 4.

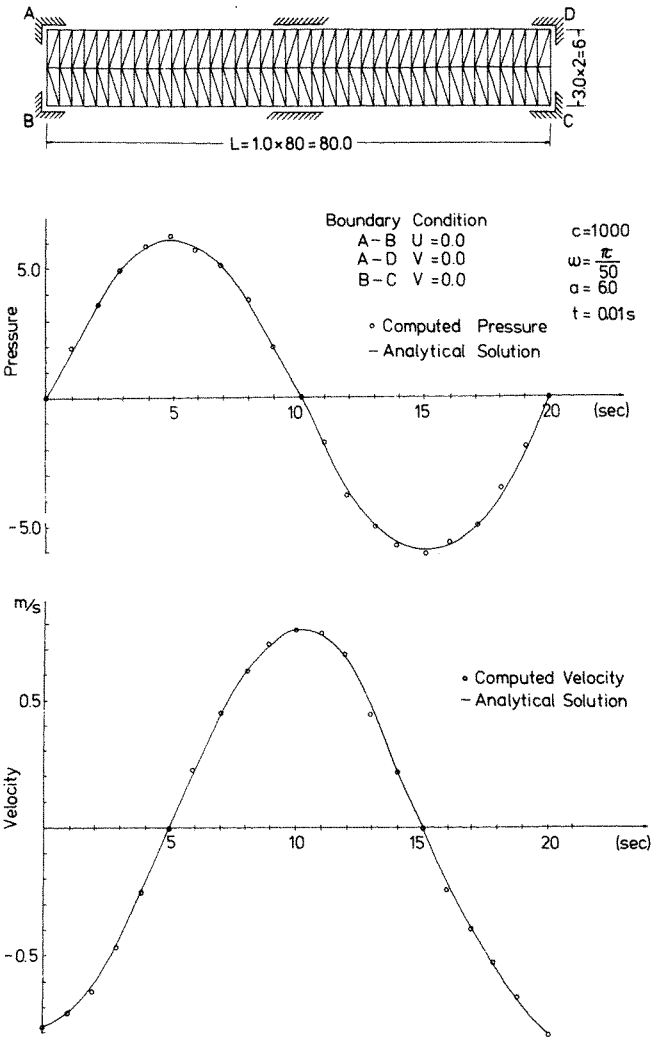

Figure 5.

The velocity and pressure can be obtained as follows.

$$P = \frac{a}{\cos\left(\frac{\omega L}{C}\right)} \cos\left\{\frac{\omega_L}{C}\left(\frac{x}{L} - \frac{x_0}{L}\right)\right\} \sin \omega t \tag{69}$$

$$v = \frac{a}{\cos\left(\frac{\omega L}{C}\right)} \sin\left\{\frac{\omega L}{C}\left(\frac{x}{L} - \frac{x_0}{L}\right)\right\} \cos \omega t \tag{70}$$

Figure 5 shows the finite element idealization and the computed results. For boundary

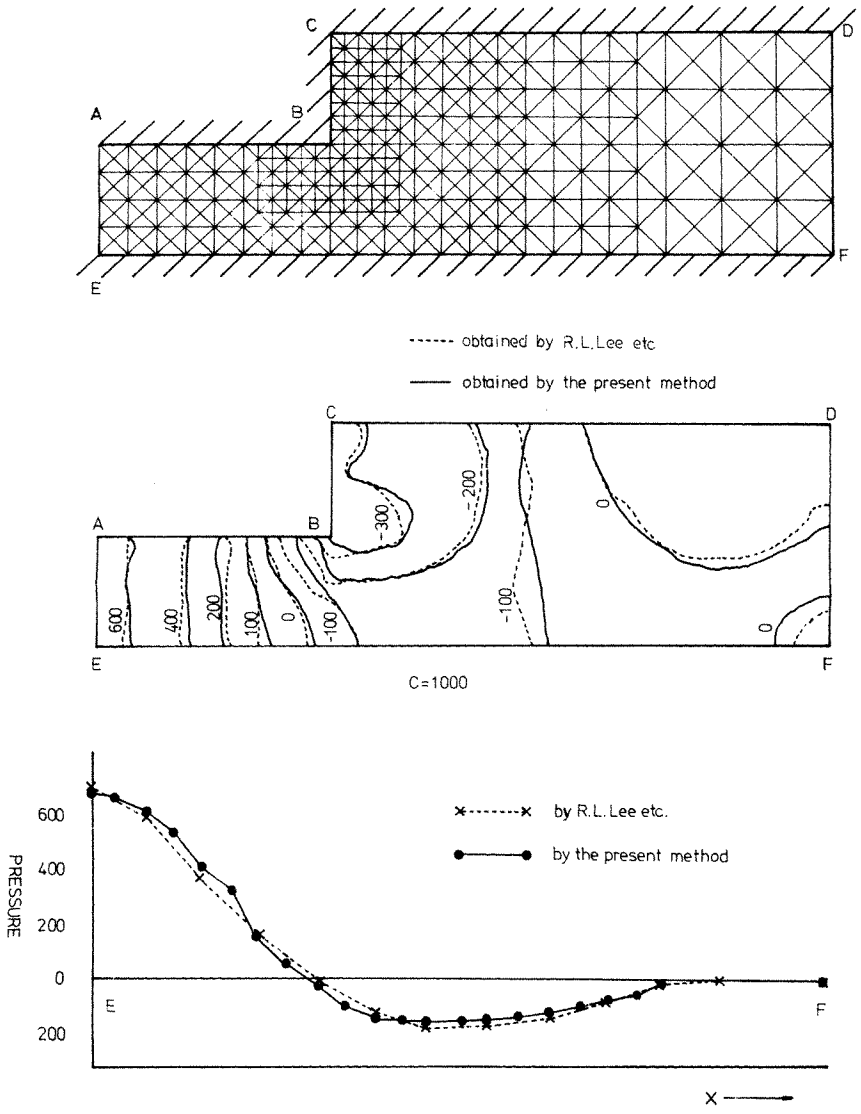

Figure 6.

conditions of velocity, the normal velocities to all boundaries are assumed zero. At the boundary C–D, the pressure is assumed to be

$$P = 6{\cdot}0 \sin\left(\frac{\pi}{50} t\right) \tag{71}$$

The speed of sound $C = 1000$ is used. The computed velocity and pressure are shown in Figure 5 compared with the analytical solution. The analytical and computed results are in close agreement. This example shows that the formulation referred to as analysis II is suitable for the computation where the pressure is given as the boundary condition.

The third example is the computation of the flow through a channel with a sudden expansion using the formulation in analysis I. The computed pressures have been compared with those obtained by Lee *et al.*[9] The finite element idealization and the boundary conditions are shown in Figure 6. At the side walls of the channel, both components of the velocity are assumed to be zero. At the entrance of the channel A–E, the parabolic velocity profile is enforced. At the boundary D–F, the surface force is assumed to be zero. A sound speed $C = 1000$ is used. The Reynolds number of the flow is $Re = 60$, where it is computed by the maximum entrance velocity and entrance length. The computed pressure, compared with the result obtained by Lee *et al.*[9] is illustrated in Figure 6. Lee *et al.* have computed the pressure by the steady flow analysis based on the penalty function formulation. Both results are in close agreement. It can be concluded from the above three examples that the present finite element method is particularly suitable for the analysis of the incompressible viscous fluid flow.

8. VORTEX SHEDDING ANALYSIS

The finite element method presented in this paper has been applied to the problem of vortex shedding behind a circular cylinder. The finite element idealization and boundary conditions employed in the analysis are shown in Figure 7. The total numbers of nodal point and finite element are 2428 and 4718, respectively. On the boundaries A–D and B–C, normal velocities to the boundary and the tangential surface force are assumed zero. On the boundary D–C, both components of the surface force are specified to be zero. A uniform velocity profile with maximum value U_0 is enforced on boundary A–B. Both components of velocity on the cylinder surface E are taken to be zero. In this analysis, the formulations in analysis I are used. Referring to air flow, sound speed and density are assumed to be $C = 337$ m/s and $\rho = 0{\cdot}1319$ kg/m^3. The volumetric viscosity κ is assumed always zero. Various values of the shear viscosity μ are used for flows of the corresponding Reynolds number. As the initial conditions, all velocities and pressures are given to be zero. The Reynolds number is estimated using the entrance velocity and diameter of cylinder as:

$$Re = \frac{\rho U_0 d}{\mu} \tag{72}$$

Three cases of the flows at the Reynolds numbers of $1{\cdot}5 \times 10^5$, $1{\cdot}5 \times 10^4$ and $1{\cdot}5 \times 10^2$ are computed. For the time increment, the estimation criteria lead to

$$\Delta T = \frac{\Delta x}{C + u_0} = 5 \times 10^{-4} \tag{73}$$

For practical computations, $\Delta T = 7{\cdot}5 \times 10^{-5}$ is employed. A selective lumping parameter $e = 0{\cdot}73$ is used.

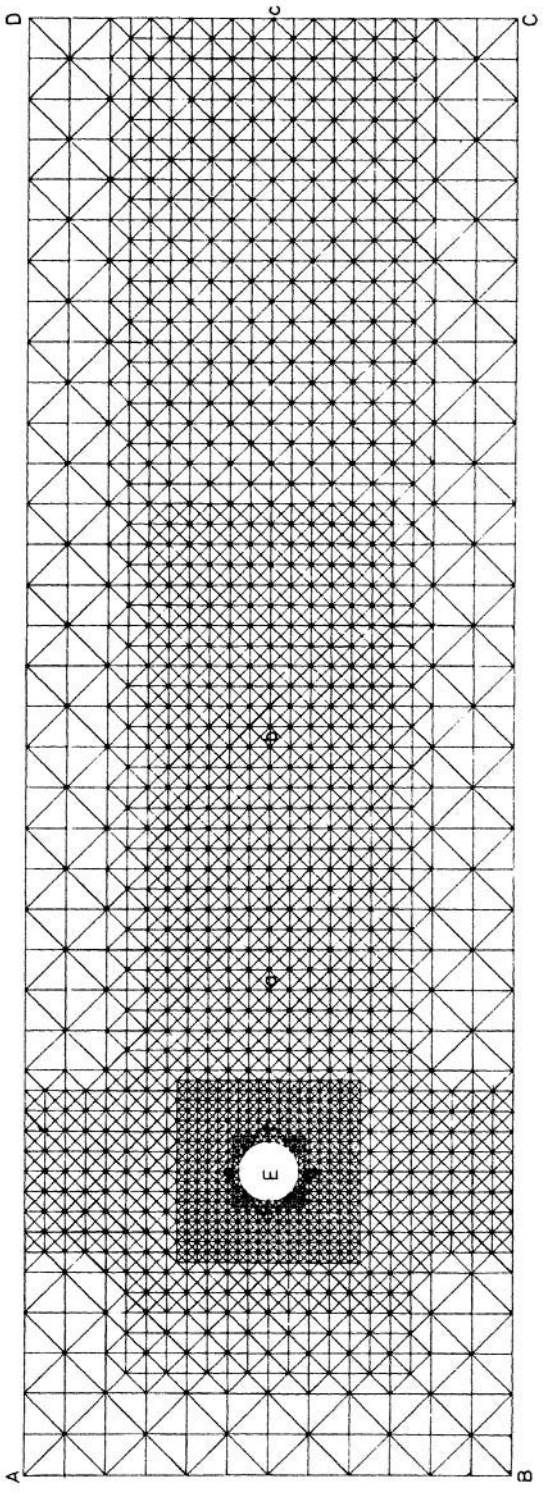

Figure 7.

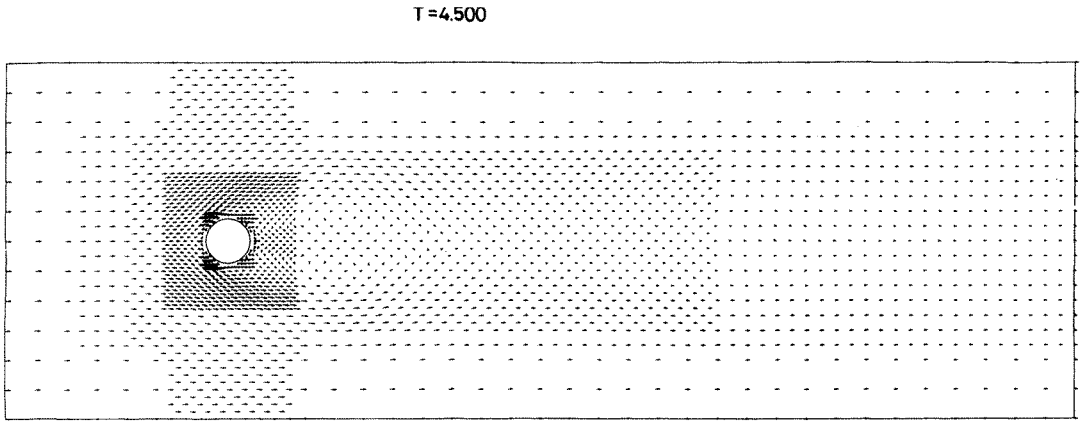

Figure 8.

In Figure 8, the computed velocity at a Reynolds numbers of 50 is presented. The computed results are symmetric. The computed velocities at Reynolds numbers of $1{\cdot}5\times10^2$, $1{\cdot}5\times10^4$ and $1{\cdot}5\times10^5$ are shown in Figures 9, 10 and 11. It is clearly illustrated in those Figures that the vortex shedding behind the cylinder can be computed exactly. It is a well known fact that the ratio a/b is always constant and independent of the Reynolds number, where a and b are the vertical and horizontal distances between vorticities, respectively. From the numerical results shown in the Figures, the convective velocity of vortex $\bar{U}$ is obtained. Using these, the Strouhal number is derived as:

$$S=\frac{\bar{U}}{U_0}\frac{d}{b} \tag{74}$$

Using the computed velocities, the ratio a/b and the Strouhal number S have been obtained and summarized in Table I.

Table I

Re	a/b	S	$1/S$
$1{\cdot}5\times10^2$	0·280	4·86	0·206
$1{\cdot}5\times10^4$	0·281	5·14	0·195
$1{\cdot}5\times10^5$	0·282	5·42	0·185

The ratio 0·280 is commonly used (e.g. Reference 24). The Strouhal number is plotted in Figure 12 with the well known experimental data.[24] The Strouhal number computed by the results by the present method is in close agreement with the experimental value. From the above investigations, it can be stated that the numerical method presented in this paper is useful for the analysis of the phenomena, such as vortex shedding behind cylinder.

Figure 13 represents velocity changing versus time at ponts a, b and c of the flow at a Reynolds number of $1{\cdot}5\times10^5$. The locations of the points are shown in Figure 7. In Figure 13, the appearance of both vertical and horizontal velocities indicates that the vertical component is more energetic close to the cylinder. Especially, the vertical component seems

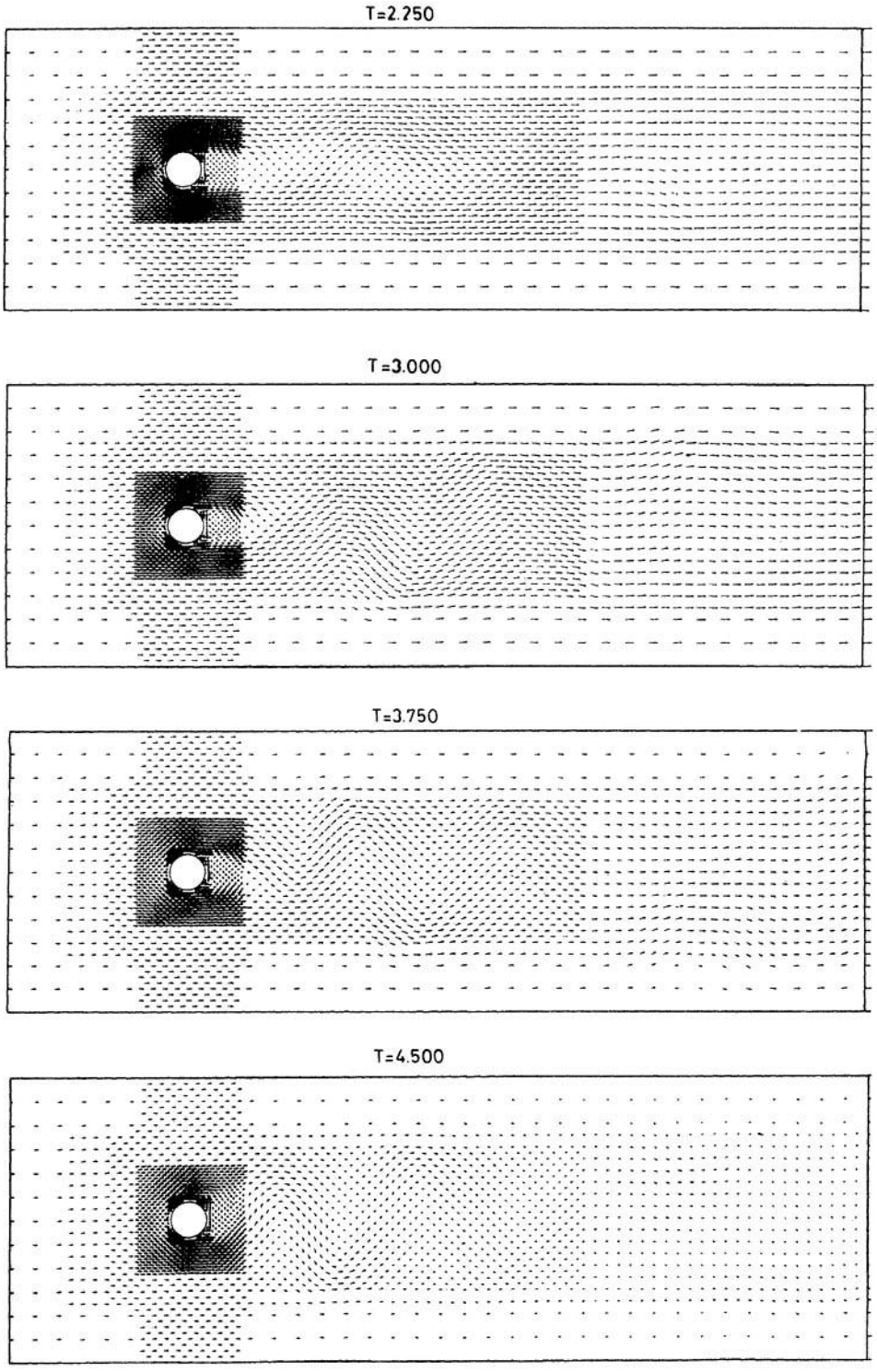

Figure 9.

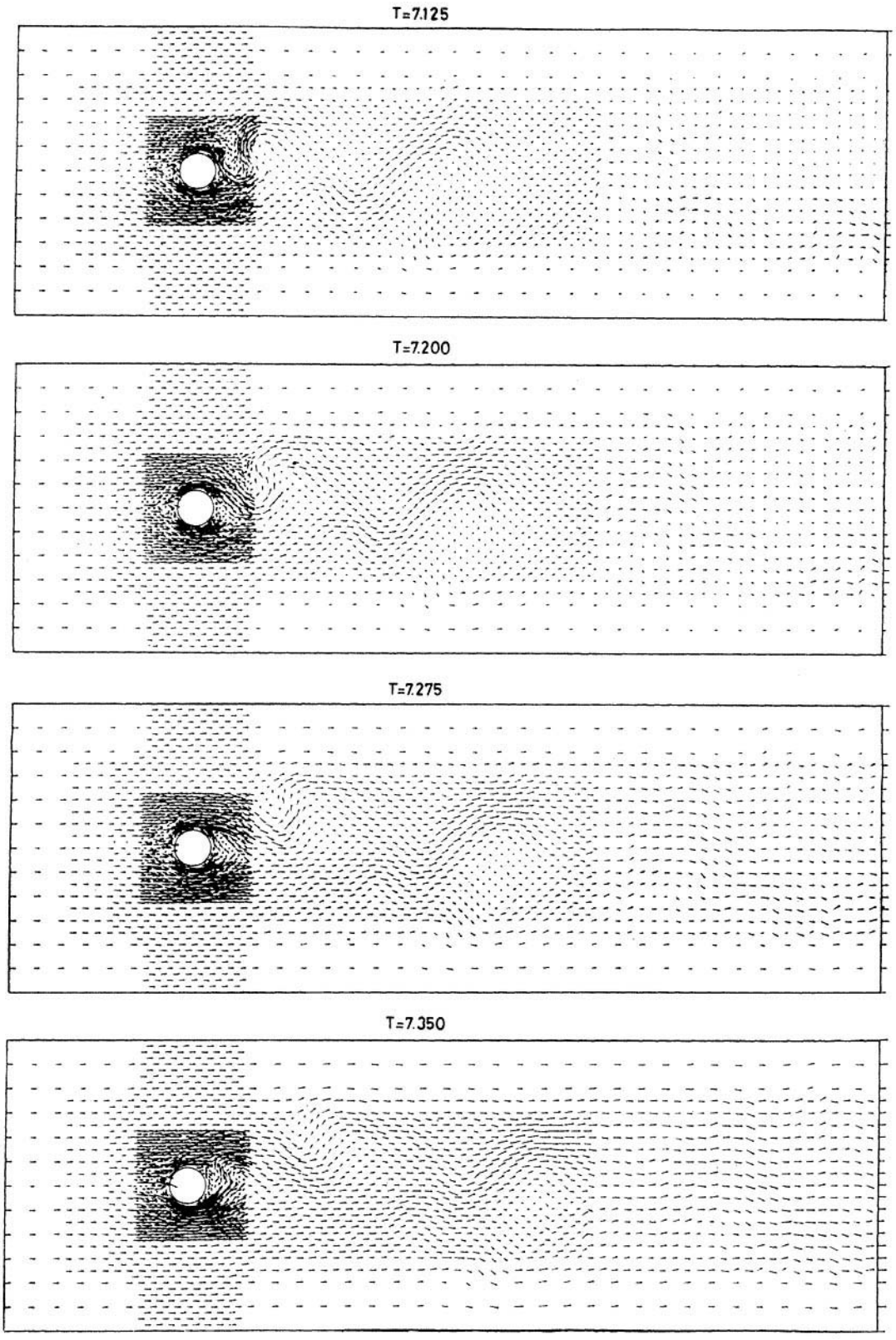

Figure 10.

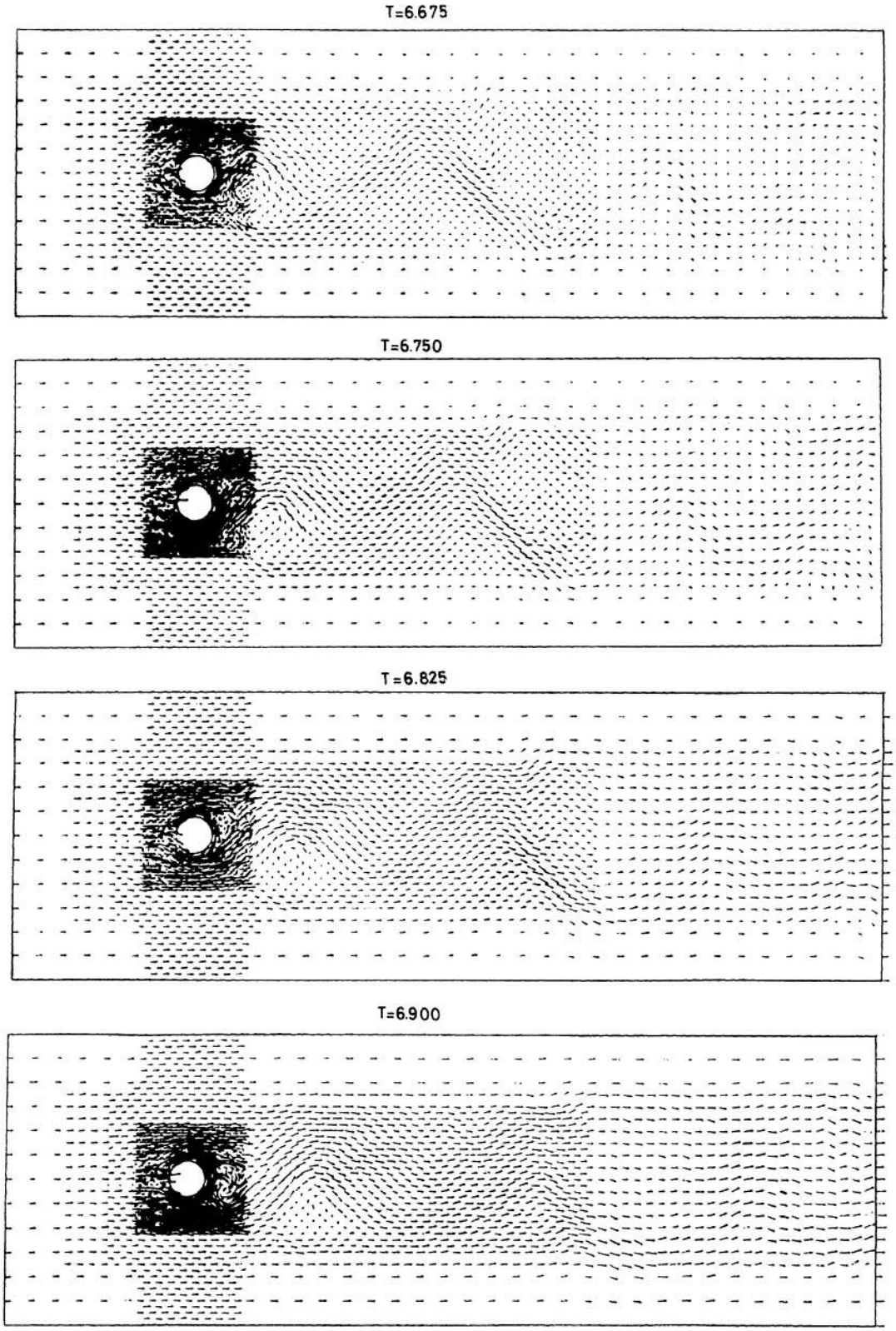

Figure 11.

$Re=1.5\times10^2$	1/S=4.86	b/a=0.280
$Re=1.5\times10^4$	1/S=5.14	b/a=0.281
$Re=1.5\times10^5$	1/S=5.42	b/a=0.282

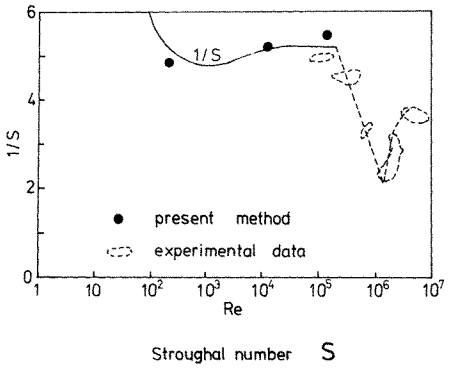

Figure 12.

zero at the boundary D–C. The period of velocity variation is given by $T=1{\cdot}8$. This seems due to the vortex.

The computed pressure at time $T=5{\cdot}775$ through $T=6{\cdot}000$ is illustrated in Figure 14. The Reynolds number is $1{\cdot}5\times10^5$. The pressure variation according to production and separation of vortex can be clearly seen. Figure 15 represents pressure variation versus time at points d, e, f and g. The period of pressure variation is $T=1{\cdot}8$. This period exactly corresponds to that of velocity shown in Figure 13.

The pressure coefficient defined by:

$$C_p=\frac{p-p_\infty}{\frac{1}{2}\rho U_0^2} \tag{75}$$

is plotted in Figure 16 at a Reynolds number of $1{\cdot}5\times10^5$. The averaged value from $T=0$ to $T=7{\cdot}5$ is used for p in equation (75). The solid line shows the well known experimental results (e.g. Ito, Miyata and Okauchi [1972]). In an average sense, the computed C_p is in reasonable agreement with the experimental value. Particularly, the computed C_p is close to the experimental value, whereas at the middle part, there is a slight discrepancy. This part is the transition domain, i.e. a substantial change in the flow can be obtained. Therefore, the finite element idealization should be fine as far as possible in this region. It is presumed that the finite element idealization should be much finer than the idealization used in this computation. The present computation has been carried out using HITAC M200H Computer of University of Tokyo. The CPU time was about 3 hours for each total computation.

9. CONCLUSION

In this paper, a finite element method of unsteady two dimensional flow of incompressible viscous fluid at high Reynolds number has been presented. The leading characteristics are summarized as follows.

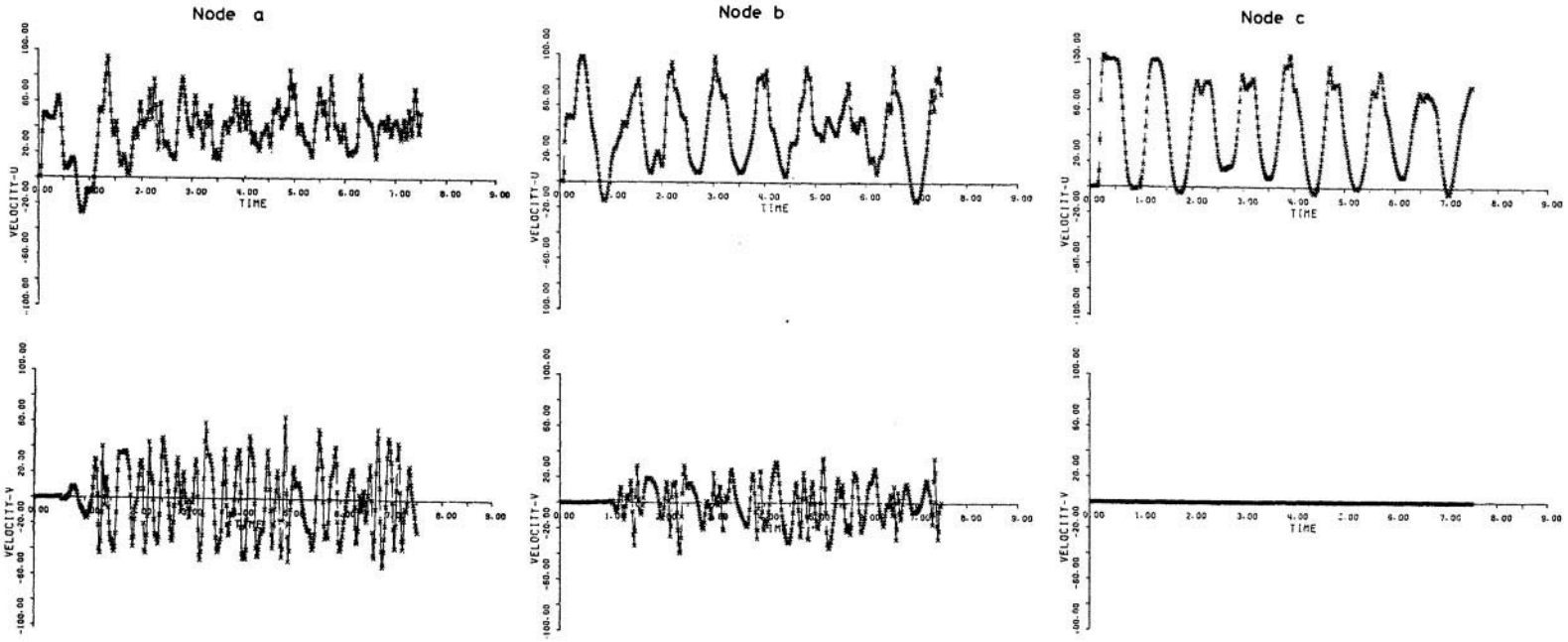

Figure 13.

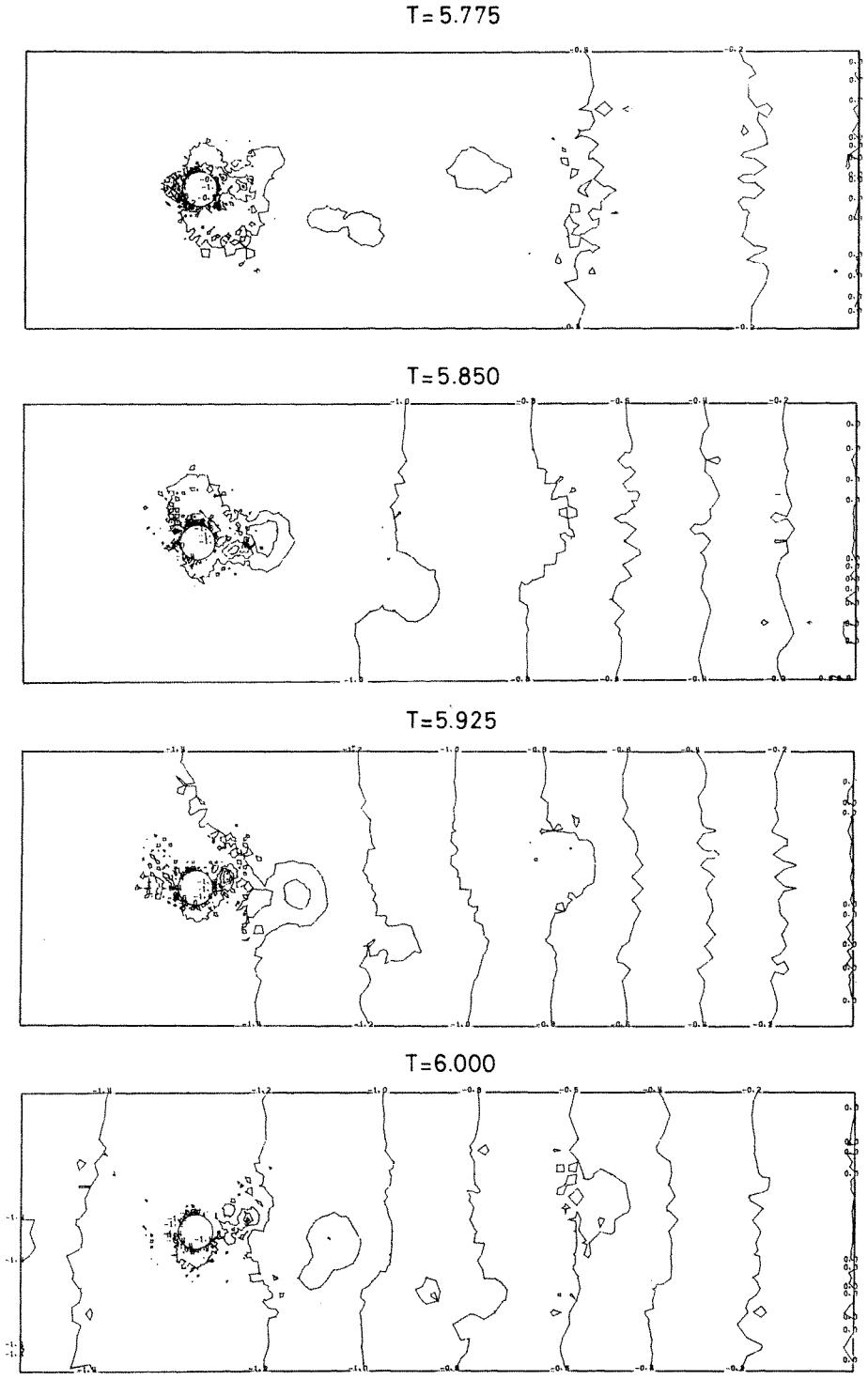

Figure 14.

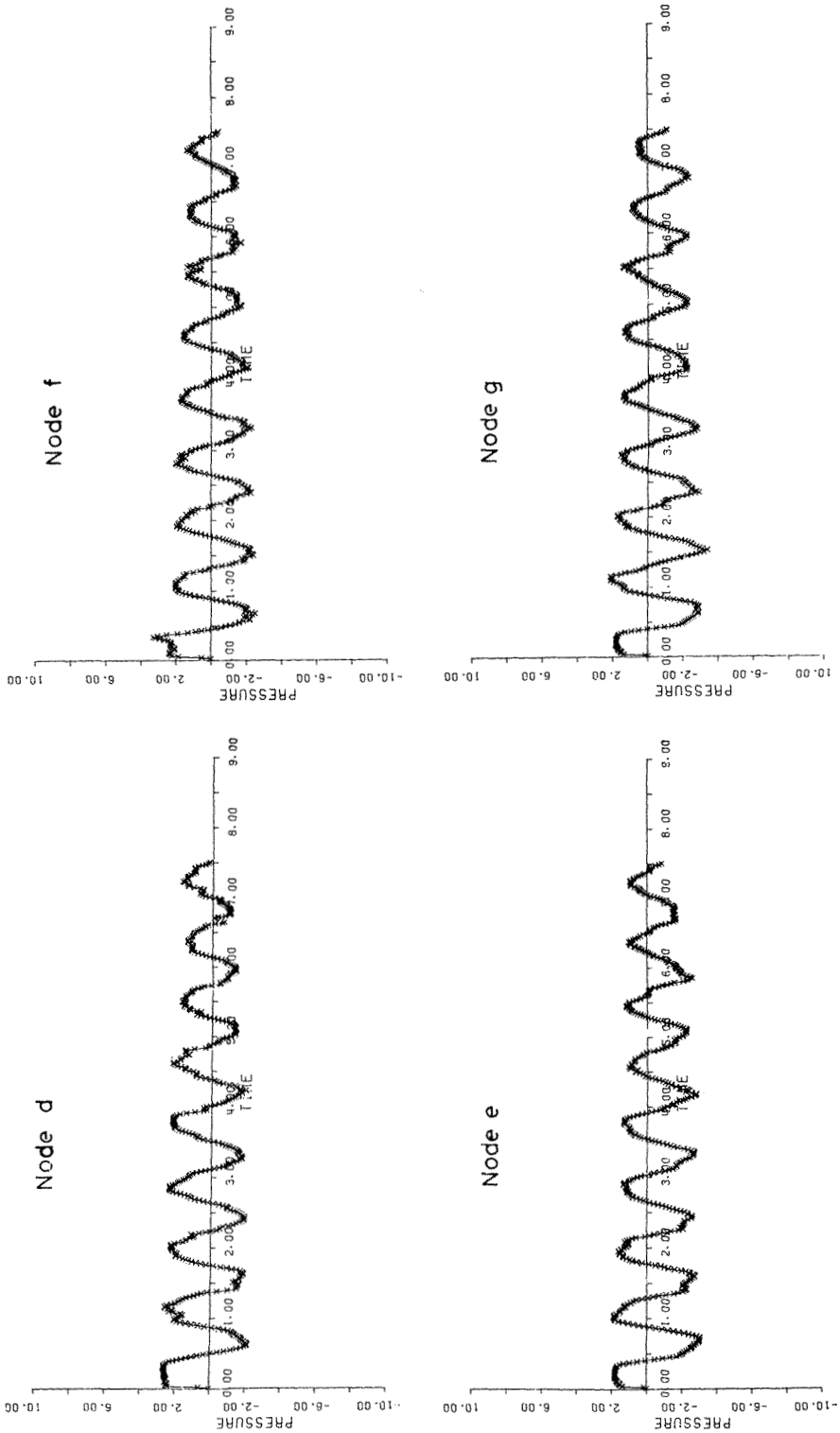

Figure 15.

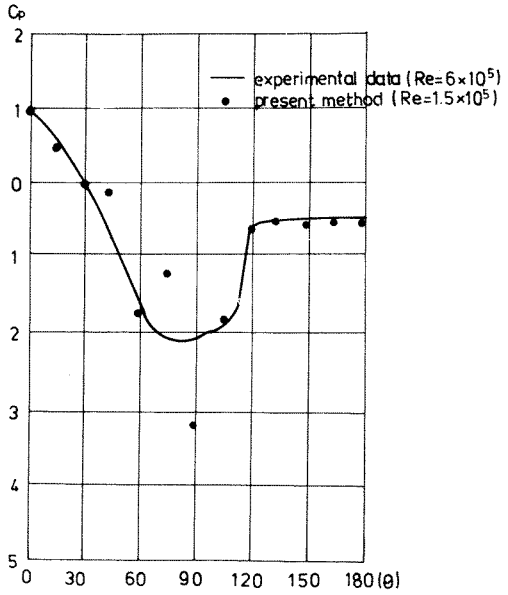

Figure 16.

(i) The basic formulation of the method is to employ slight compressibility. The equation of state has been transformed into the improved form of the equation of continuity using the speed of sound. Using this equation, an explicit scheme in time has been established. The equation corresponds to the physical interpretation of the penalty function method.

(ii) For the numerical integration in time, the two step explicit scheme based on the linear triangular finite element has been employed. Using the explicit scheme, the requirements for core storage and for computational time can be considerably reduced.

(iii) The practical criterion for the selection of the time increment is expressed as:

$$\Delta t \leqq \alpha \frac{\Delta x}{U+C}$$

where $\alpha = 0{\cdot}1 \sim 0{\cdot}3$.

(iv) A comparison of the numerical results obtained by the present method with the results computed by the analytical and the conventional numerical methods has been presented. The results are in close agreement.

(v) The flow passed cylinder has been computed at Reynolds numbers of $1{\cdot}5 \times 10^2$, $1{\cdot}5 \times 10^4$ and $1{\cdot}5 \times 10^5$. The vortex shedding has clearly been computed. The Strouhal number is comparable with the experimental data.

(vi) The pressure coefficient computed by the present method has been compared with the coefficient obtained by experiments. There seems to be a considerable discrepancy, which is assumed to originate from the use of insufficient finite elements in the idealization.

For the computation of the flow at relatively high Reynolds numbers, it is necessary to use refined finite element idealization and short time increment. In this sense, the explicit

numerical integration scheme is preferable when considering core storage and computational time. For the numerical integration in time, the selective lumping two step scheme based on linear triangular finite element is suitable from the point of numerical stability. A part of this research has been submitted to the proceedings of Japan Society of Civil Engineers.[23]

REFERENCES

1. T. J. R. Hughes, R. L. Taylor and J. Levy, 'High Reynolds number, steady, incompressible flows by a finite element method Gallagher *et al.* (eds.) in Finite Elements in Fluids, Vol. 3, Wiley, 1978.
2. T. J. R. Hughes, W. K. Liu, and A. Brooks, 'Finite element analysis of incompressible viscous flows by the penalty function formulation', *J. Computational Phys.*, **30,** 1–60 (1979).
3. J. C. Heinrich, R. S. Marshall and O. C. Zienkiewicz, 'Penalty function solution of coupled convective and conductive heat transfer, C. Taylor *et al.* (eds.) in *Numerical Methods in Laminar and Turbulent Flow*, Pentech Press, 935–946 (1978).
4. J. N. Reddy, 'On the finite element method with penalty for incompressible fluid flow problems', J. R. Whiteman (ed.) in *The Mathematics of Finite Elements and Applications III*, Academic Press, 227–235 (1979).
5. J. N. Reddy, 'On the mathematical theory of penalty–finite elements for Navier–Stokes equations', *Proceedings of the Third International Conference on Finite Elements in Flow Problems*, University of Calgary, 146–154 (1980).
6. J. T. Oden, 'Penalty methods and selective reduced integration for Stokesian flows', *Proceedings of the Third International Conference on Finite Elements in Flow Problems*, University of Calgary, 140–154 (1980).
7. R. Temam, 'Sur l'approximation de la solution des equations de Navier–Stokes par la methode des pas franctionnaries (I)', *Arch. Rati. Mech. Anal.*, **32,** 135–153 (1969).
8. R. Temam, 'Navier–Stokes equations', J. L. Lions *et al.* (eds.) in *Studies in Mathematics and Its Applications*, North Holland, 1977.
9. R. L. Lee, P. M. Gresho and R. L. Sani, 'Smoothing techniques for certain primitive variable solutions of Navier–Stokes equations', *Int. J. Num. Meth. Engng.*, **14,** (12), 1785–1804 (1979).
10. R. L. Lee, P. M. Gresho, S. T. Chan and R. L. Sani, 'A comparison of several conservative forms for finite element formulations of the incompressible Navier–Stokes or Boussinesq equations', *Proceedings of the Third International Conference on Finite Element Method in Flow Problems*, Banff, University of Calgary, 236–227 (1980).
11. P. M. Gresho, R. L. Lee and C. D. Upson, 'FEM solution of the Navier–Stokes equations for vortex shedding behind a cylinder: experiments with the four node element', S. Y. Wang *et al.* (eds.), in *Finite Elements in Water Resources*, University of Mississippi, 4.48–4.65 (1980).
12. A. J. Chorin, 'A numberical method for solving incompressible viscous flow problems', *J. Computational Phys.*, **2,** 12–26 (1967).
13. G. Marshall and E. Van Spiegel, 'On the numerical treatment of the Navier–Stokes equations for an incompressible fluid', *J. Engng. Math.*, **7,** (2), 173–188 (1973).
14. C. W. Hirt and B. D. Nichols, 'Adding limited compressibility to incompressible hydrocodes', *J. Computational Phys.*, **34,** 390–400 (1980).
15. M. Kawahara, 'Convergence of finite element Lax–Wendroff method for linear hyperbolic differential equation', *Proc. J.S.C.E.*, **253,** 95–207 (1976).
16. M. Kawahara, N. Takeuchi and T. Yoshida, 'Two step explicit finite element method for Tsunami wave propagation analysis', *Int. J. Num. Meth. Engng.*, **12,** 331–351 (1978).
17. M. Kawahara, 'Steady and unsteady finite element analysis of incompressible viscous fluid', R. H. Gallagher, O. C. Zienkiewicz, J. T. Oden, M. M. Cecchi and C. Taylor (eds.) in *Finite Elements in Fluids*, Vol. 3, pp. 23–54, Wiley, 1978.
18. M. Kawahara, 'On finite element methods in shallow water long wave flow analysis', J. T. Oden (ed.) in *Computational Methods in Nonlinear Mechanics*, North-Holland, 261–187 (1980).
19. M. Kawahara and T. Yokoyama, 'Finite element method for direct runoff flow', *Proc. A.S.C.E.*, **106,** (HY4), 519–534 (1980).
20. M. Kawahara, S. Nakazawa, S. Ohmori and T. Takagi, 'Two-step explicit finite element method for storm surge propagation analysis', *Int. J. Num. Meth. Engng.*, **15,** 1129–1148 (1980).
21. M. Kawahara and K. Hasegawa, 'SEADASER—A general purpose finite element program for coastal sea current and dispersion', *Advances in Engng. Software*, **3,** (1), 2–8 (1980).
22. M. Kawahara, H. Hirano, K. Tsubota and K. Inagaki, 'Selective lumping finite element method for shallow water flow', *Int. J. Num. Meth. Fluid.*, **2,** 89–112 (1982).
23. M. Kawahara and H. Hirano 'Two step explicit finite element method for high Reynolds number viscous fluid flow', (submitted to *Proc. J.S.C.E.*)
24. M. Ito, I. Okauchi and T. Miyata, 'Wind resisted structures' Maruzen (in Japanese).